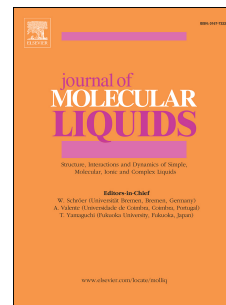


# Journal Pre-proof

The effect of the position of chiral (–)-menthyl on the formation of blue phase and mesophase behavior in biphenyl-benzoate liquid crystals

Zhang-Pei Chen, Xin-Jiao Wang, Ling-Xin Meng, Ji-Wei Wang, Ying-Gang Jia



PII: S0167-7322(19)32090-2

DOI: <https://doi.org/10.1016/j.molliq.2019.112003>

Reference: MOLLIQ 112003

To appear in: *Journal of Molecular Liquids*

Received Date: 12 April 2019

Revised Date: 23 October 2019

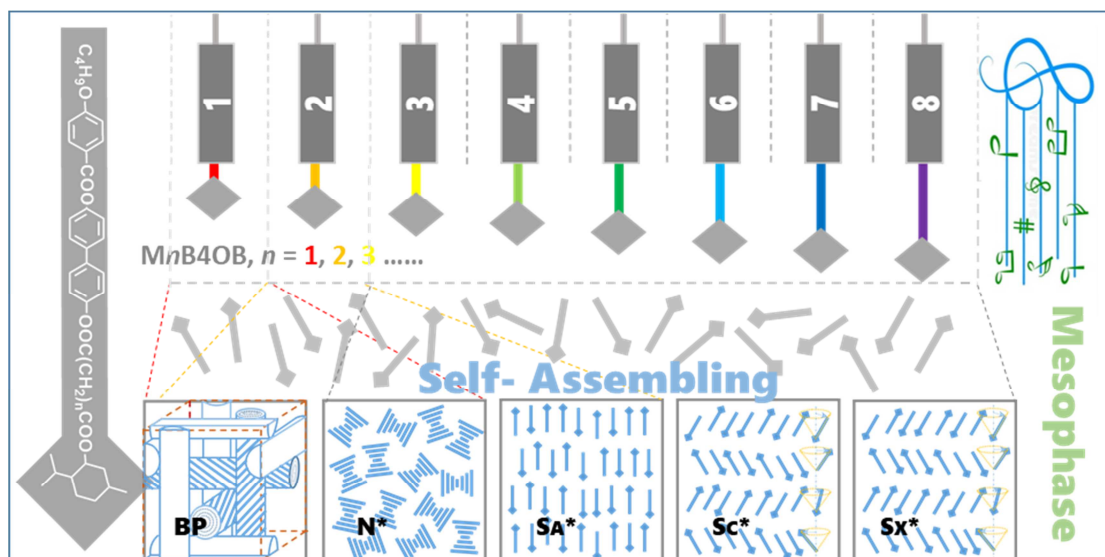
Accepted Date: 23 October 2019

Please cite this article as: Z.-P. Chen, X.-J. Wang, L.-X. Meng, J.-W. Wang, Y.-G. Jia, The effect of the position of chiral (–)-menthyl on the formation of blue phase and mesophase behavior in biphenyl-benzoate liquid crystals, *Journal of Molecular Liquids* (2019), doi: <https://doi.org/10.1016/j.molliq.2019.112003>.

This is a PDF file of an article that has undergone enhancements after acceptance, such as the addition of a cover page and metadata, and formatting for readability, but it is not yet the definitive version of record. This version will undergo additional copyediting, typesetting and review before it is published in its final form, but we are providing this version to give early visibility of the article. Please note that, during the production process, errors may be discovered which could affect the content, and all legal disclaimers that apply to the journal pertain.

© 2019 Published by Elsevier B.V.

# The effect of position of chiral (-)-menthyl on the formation of blue phase and mesophase behavior in biphenyl-benzoate liquid crystals



# The effect of the position of chiral (-)-menthyl on the formation of blue phase and mesophase behavior in biphenyl-benzoate liquid crystals

Zhang-Pei Chen<sup>1</sup>, Xin-Jiao Wang<sup>1</sup>, Ling-Xin Meng<sup>1</sup>, Ji-Wei Wang<sup>2,3\*</sup>, Ying-Gang Jia<sup>1\*</sup>

<sup>1</sup>*Department of Chemistry, College of Science, Northeastern University, Shenyang, 110819, P. R. China*

<sup>2</sup>*Fujian Provincial Key Laboratory of Featured Materials in Biochemical Industry, College of Chemistry and Materials, Ningde Normal University, Ningde, 352100, P. R. China*

<sup>3</sup>*Fujian Province University Engineering Research Center of Mindong She Medicine, College of Chemistry and Materials, Ningde Normal University, Ningde, 352100, P. R. China*

## Abstract

Eight new chiral liquid crystal compounds 4-(4-menthyloxy-*n*-oxoalkanoyloxy) biphenyl-4'-yl 4-butoxybenzoates **M<sub>n</sub>B4OB** ( $n = 1-8$ ), were prepared by modifying the position of chiral (-)-menthyl in the menthol based liquid crystal compounds through gradually increasing the alkyl chain length of the dicarboxylic spacer. All compounds were characterized by FT-IR and NMR spectroscopy in order to prove their chemical structures. Differential scanning calorimetry (DSC), polarized optical microscopy (POM) and X-ray diffraction were carried out to systematically investigate their phase transition behaviors. The position of chiral (-)-menthyl in relation to the core has a great effect on the formation of BPs and mesomorphic behaviors. Only CLCs **M1B4OB** and **M2B4OB** with short spacer chains

---

\*Corresponding author: jiayinggang@mail.neu.edu.cn (Y.G. Jia), jlwjw@sina.com (J. W. Wang)

presented blue phases. Furthermore, the length and parity of the flexible spacers have a profound influence on phase structures and phase transition behaviors. An odd-even effect is observed for these chiral liquid crystal compounds.

**Keywords:** Chiral liquid crystal, Spacer length, Blue phases, Odd-even effect, (-)-Menthol

## 1. Introduction

Liquid crystals (LCs) formed by self-assembly of the anisotropic molecules represent a distinct and interesting state of matter exhibiting both liquid-like fluidity and crystal-like order. This unique feature leads to self-healing, adaptive, and stimuli-responsive behaviors of supramolecular systems, which enable LCs to be used as the typical self-organizing molecular materials in the modern material science [1-4]. Chiral molecules have no plane of symmetry and are optically active. Molecular asymmetry imposes a reduction in the space symmetry, which leads to multitudinous chiral liquid crystalline phase, such as cholesteric ( $N^*$ ), chiral smectic  $Sm^*$ , twist grain boundary, and cubic blue phases (BPs), each with unprecedented and unique properties [1, 2]. In these chiral mesophases, BPs possess a cubic lattice structure, which can be regarded as a self-organized three-dimensional (3D) photonic crystal. Indeed, BPLCs have attracted considerable attention from a wide range of applications across numerous fields [5-7]. BPs have been known to consist of doublet-twist cylinders (DTCs) and can be classified as BPI, BPII and BPIII in light of their emergence order [8]. Both BPI and BPII have a fluid three-dimensional periodic structure with body-centered cubic and simple cubic symmetry, respectively. In contrast, BPIII is amorphous or isotropic symmetry with an arbitrary orientation [9-11]. In recent years, BPs have been widely investigated due to their potential applications such as display devices, tunable photonic crystals, photonic band-gap

materials etc. [12-15]. Therefore, numerous efforts have been made towards the development of BPLC materials through rational molecular design and efficient synthetic methods [16-18].

Previous studies have demonstrated that the liquid-crystal morphologies or mesogenic behaviors of LCs strongly depend on their molecular structures, and even could be oriented to a large extent by altering the numbers, size, and polarity of rigid cores as well as the length and parity of the spacers [19]. In BPs, the peculiar structures depend on how the LC molecules self-assemble into DTC structures and pack them to fill the space. Until now, a lot of BPLCs have been prepared and their physical properties have been investigated. Chirality is regarded as a very important factor responsible for the appearance of BPs with DTC structure. Generally, there are two popular methods to prepare LCs with BPs. The first one is to develop single-component mesogen with short-pitch by introducing chiral reagents into mesogenic cores. The second strategy is to utilize the host-guest approach by adding chiral guest into an LC host. When chirality in the host-guest system is high enough, which has a high twisting power [20, 21]; the chiral molecule can drive LC molecules into DTC structure. Even though doping is a simple and often used method for the preparation of BPLCs, a single-component LC with wide temperature interval of BPs and the studies on the structure-property correlations still attract many researchers.

BPs are frustrated defect phases, generally observed between the isotropic phase and the cholesteric phase of highly chiral mesogen with short pitch [22]. Optically active (-)-menthol shows a large specific rotation, and normally is utilized as a guest to induce cholesteric phases [23, 24]. Due to the bulky menthyl group being a terminal group directly linked to the phenyl rings, no BPs or mesophase were observed for them. Recently, we have successfully synthesized chiral liquid crystal compounds based on (-)-menthol by introducing the

oxyacetyloxy spacer (-OCH<sub>2</sub>COO-) or butanedioxyloxy spacer (-OOCCH<sub>2</sub>CH<sub>2</sub>COO-) between the mesogenic core and the bulky terminal menthyl moiety and they all reveal BP phases [25-31]. The spacer made menthyl unbound to mesogenic core and imparts molecular chirality to mesophase leading to the formation of BPs. In those studies, the effects of terminal chain length and structure of mesogenic core on BPs were further discussed in details [29-31]. We found that in those (-)-menthol-derived CLCs, the chirality of (-)-menthol can lead to the formation of BPs, and terminal chain length and structure of mesogen did not affect BPs formation except the temperature range of BPs. However, when hexanedioxyloxy group acted as a linking unit between mesogenic core and chiral (-)-menthyl, no BPs were formed [32]. Thus, we changed the location of chiral (-)-menthyl with respect to the rigid core by varying the linking spacers from butanedioxyloxy to decanedioxyloxy and found that the length of the flexible spacers has a great effect on the formation of BPs and mesomorphic behaviors [33]. In connection, how the effect of propanedioxyloxy as a new spacer together with those spacers mentioned above on the formation of BP, mesomorphic behavior, and molecules arrangement is what we consider in this paper.

Firstly, by modifying the position of chiral (-)-menthyl in relation to the mesogenic core *via* spacer length, a new homologous CLCs with chiral (-)-menthol as chiral origin, butoxy as one terminal group, biphenyl-benzoate as core, was designed. Through gradually increasing the alkyl chain length of the alkanedioxyloxy spacer (from propanedioxyloxy to decanedioxyloxy) between chiral (-)-menthyl and mesogenic core, eight new CLC compounds: 4-(4-menthyloxy-*n*-oxoalkanoyloxy)biphenyl-4'-yl 4-butoxybenzoates **M<sub>n</sub>B4OB** (*n* = 1-8) were prepared, where *n* indicates the number of carbon atoms in the flexible spacers. The mesomorphism and thermal behavior of these compounds were investigated by differential

scanning calorimeter (DSC), POM and XRD. The selective reflection of light was studied with UV. The effect of flexible spacers of varying length and parity on the formation of BPs, and mesomorphic properties has been discussed systemically.

## 2. Experimental section

### 2.1. Materials

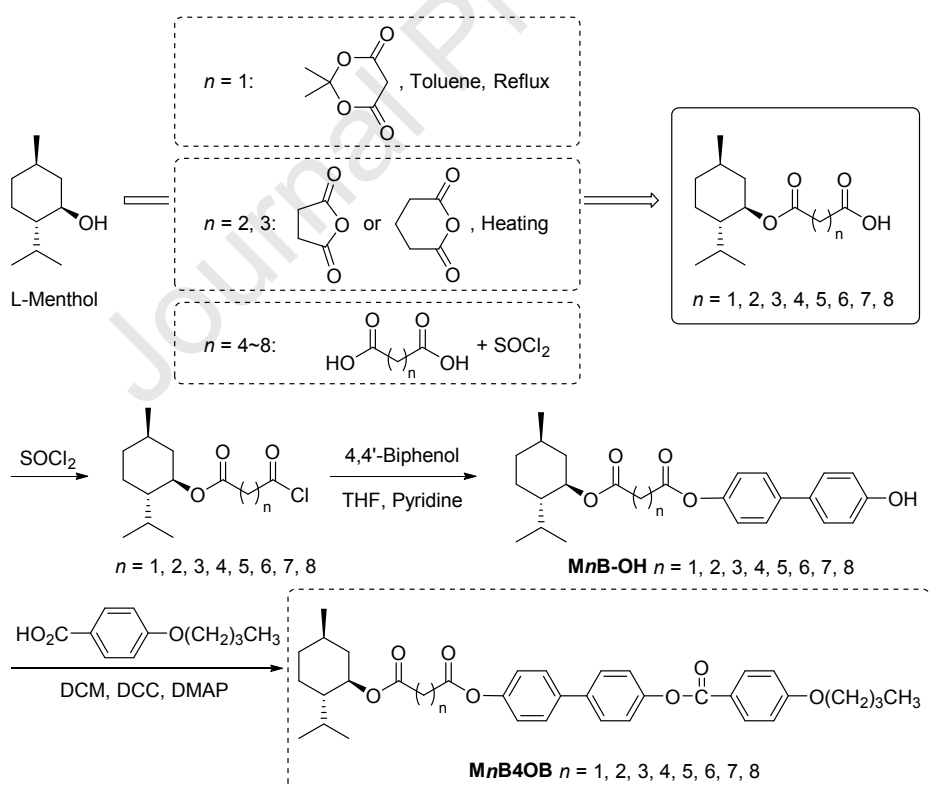
All chemicals were obtained from the indicated sources. (-)-Menthol was purchased from Shanghai Kabo Chemical Co. (China). 2,2-Dimethyl-1,3-dioxane-4,6-dione was purchased from Tianjin Bodi Chemical Co., Ltd. (Tianjin, China). Succinic anhydride, glutaric anhydride, adipic acid, pimelic acid, suberic acid, azelaic acid, and sebacic acid were purchased from Sinopharm Chemical Reagent Co., Ltd (China). All other reagents and solvents were purchased from Tianjin Bodi Chemical co., Ltd. (Tianjin, China). The reagents were used directly without further purification. The solvents were purified by standard methods. The purities of all intermediates and LC compounds were checked with column chromatography using TLC sheets coated with silica gel. All the CLC compounds were recrystallized from methanol.

### 2.2. Characterization

FT-IR spectra were measured with the samples pressed into KBr pellets on a PerkinElmer spectrum One (B) spectrometer. NMR spectra were performed on Bruker ARX 600 MHz or 300 MHz (Bruker, Karlsruhe, Germany) NMR spectrometer, and tetramethylsilane (TMS) was used as an internal standard to report chemical shifts in ppm. Element analysis (EA) was performed by use of an Elementar Vario ELIII (Elementar, Germany). The thermal behavior

was determined with a Netzsch 204 DSC (Netzsch, Hanau, Germany) with a heating and cooling rate of 10 °C/ min in a nitrogen atmosphere. The LC optical textures were observed and recorded with a Leica DMRX POM (Leica, Wetzlar, Germany) equipped with a Linkam THMSE-600 (Linkam, London, UK) cool and hot stage. X-ray diffraction (XRD) measurements were performed using a nickel-filtered Cu-K $\alpha$  ( $\lambda = 1.542 \text{ \AA}$ ) radiation monochromatised with a Rigaku DMAX-3A powder diffractometer (Rigaku, Japan). The samples were filled individually into two different Lindemann capillary (1 mm diameter) tubes and both the ends of the tubes were flame-sealed. The selective reflection wavelength was measured using a PerkinElmer 950 ultraviolet/visible spectrometer with a hot stage.

### 2.3. Synthesis of the chiral compounds



**Scheme 1.** Synthetic route of CLC compounds **MnB4OB**.

Scheme 1 shows the chemical structures and synthetic routes of the CLCs with different

lengths of the flexible spacers. All the intermediates and compounds gave single spots on thin layer chromatography and NMR spectra, which are in agreement with their structures. The detailed synthesis steps of **MnB4OB** ( $n = 1-8$ ) are described below.

### 2.3.1. Synthesis of the intermediates (**MnB-OH**)

#### 2.3.1.1 Synthesis of the intermediates (**M1B-OH**)

(-)-Menthol (1.2g, 7.67 mmol) and 2,2-dimethyl-1,3-dioxane-4,6-dione (1.1 g, 7.63 mmol) were placed into a 50-mL round-bottom flask, then 8 mL of toluene was added. The mixture was stirred at reflux for 20 h. After completion of the reaction (checked by TLC with iodine), the reaction mixture was cooled to room temperature and concentrated. The obtained residue was applied onto a silica gel column with ethyl acetate/petroleum ether (40:60/v:v) to achieve 3-(menthyloxy)-3-oxopropanoic acid as a colorless oil (1.0 g, 54%).  $^1\text{H}$  NMR (300 MHz, Chloroform-*d*)  $\delta$  4.72 (m, 1H), 3.41 (s, 2H), 2.07-0.93 (m, 9H), 0.90 (dd,  $J = 7.4, 5.6$  Hz, 6H), 0.75 (d,  $J = 6.9$  Hz, 3H).

The 3-(menthyloxy)-3-oxopropanoic acid (2.144 g, 8.8 mmol) and thionyl chloride (10.0 mL) were added into a round flask. The mixture was stirred at 64 °C for 3 h. After removal of the excess thionyl chloride *via* distillation under reduced pressure, the intermediate compound (-)-menthyl malonyl chloride was obtained. Then, this intermediate was dissolved in 20 mL of anhydrous tetrahydrofuran (THF) and was added dropwise to a solution of 4,4'-dihydroxybiphenyl (1.966 g, 10.5 mmol) in 10 mL THF and 0.85 mL pyridine. The result reaction mixture was stirred at room temperature for 3 h. After evaporation of the solvent, the crude product was purified by column chromatography on silica gel (200-300 mesh), with petroleum ether-ethyl acetate (80:20/v:v) as the eluent, to afford pure white solid **M1B-OH**

(2.015 g, 56%). IR (KBr,  $\text{cm}^{-1}$ ): 3515 (-OH), 2952, 2932, 2864 (-CH<sub>3</sub>, -CH<sub>2</sub>-), 1747, 1724 (-COO-), 1497 (Ar-), 1207, 1171 (C-O-C), 831 (Ar-H). <sup>1</sup>H NMR (300 MHz, Chloroform-*d*)  $\delta$  7.59-7.48 (m, 2H), 7.46-7.37 (m, 2H), 7.20-7.06 (m, 2H), 6.95-6.80 (m, 2H), 4.91 (s, 1H), 4.81 (td,  $J = 10.9, 4.4$  Hz, 1H), 2.17-1.82 (m, 2H), 1.70 (d,  $J = 12.1$  Hz, 2H), 1.52-0.37 (m, 16H).

### 2.3.1.2 Synthesis of the intermediates **M2B-OH** and **M3B-OH**

4-(Menthyloxy)-4-oxobutanoic acid and intermediates **M2B-OH** were synthesized according to the previous reported procedure [29]. Similarly, 5-(menthyloxy)-5-oxopentanoic acid and intermediates **M3B-OH** were prepared according to the synthesis method of 4-(menthyloxy)-4-oxobutanoic acid and compound **M2B-OH**, respectively. The detailed data of **M2B-OH** and **M3B-OH** are given in ESI.

### 2.3.1.3 Synthesis of the intermediates **MnB-OH** ( $n = 4, 5, 6, 7, 8$ )

Intermediates **MnB-OH** ( $n = 4, 5, 6, 7, 8$ ) were synthesized from (-)-menthol and the corresponding aliphatic dicarboxylic acid with similar methods to our previous paper [32]. The detailed data of **MnB-OH** ( $n = 4, 5, 6, 7, 8$ ) were showed in ESI.

### 2.3.2. Synthesis of liquid crystal compounds (**MnB4OB**)

4-Butoxybenzoic acid (1.8 mmol), intermediate **M1B-OH** (1.8 mmol), DCC (1.8 mmol) and DMAP (0.010 mmol) were dissolved in 20 mL methylene chloride. The reaction mixture was stirred at room temperature for 24 h. After the precipitation dicyclohexylurea (DCU) was removed by filtration; the filtrate was washed with dilute HCl aqueous solution, water, dried over anhydrous MgSO<sub>4</sub>, and then concentrated under reduced pressure. The crude product was purified by column chromatography on silica gel (200-300 mesh), with hexane-ethyl

acetate (4:1/v:v) as the eluent, to yield a pure white powder **M/B4OB** (yield 43%). IR (KBr,  $\text{cm}^{-1}$ ): 2956-2869 (-CH<sub>3</sub>, -CH<sub>2</sub>-), 1762, 1740, 1732 (-COO-), 1606, 1510 (Ar-), 1209, 1167 (C-O-C), 847 (Ar-H). <sup>1</sup>H NMR (600 MHz, Chloroform-*d*)  $\delta$  8.17-8.15 (d, *J* = 8.9 Hz, 2H), 7.62-7.57 (m, 4H), 7.28 (d, *J* = 8.6 Hz, 2H), 7.19 (d, *J* = 8.6 Hz, 2H), 6.98 (d, *J* = 8.9 Hz, 2H), 4.82 (td, *J* = 10.9, 4.4 Hz, 1H), 4.06 (t, *J* = 6.5 Hz, 2H), 3.62 (s, 2H), 2.10-2.07 (m, 1H), 1.96 (td, *J* = 7.0, 2.7 Hz, 1H), 1.84-1.79 (m, 1H), 1.70 (dt, *J* = 12.1, 2.9 Hz, 2H), 1.56 (d, *J* = 2.7 Hz, 1H), 1.52 (qd, *J* = 9.2, 8.4, 6.5 Hz, 3H), 1.44 (ddt, *J* = 14.4, 10.8, 3.1 Hz, 1H), 1.12-1.03 (m, 2H), 1.00 (t, *J* = 7.4 Hz, 3H), 0.91 (dd, *J* = 13.0, 6.8 Hz, 7H), 0.79 (d, *J* = 6.9 Hz, 3H). <sup>13</sup>C NMR (100 MHz, Chloroform-*d*)  $\delta$  165.7 (C=O), 165.3 (C=O), 165.0 (C=O), 163.6 (C), 150.6 (C), 149.9 (C), 138.6 (C), 137.9 (C), 132.3 (CH), 128.3 (CH), 128.2 (CH), 122.2 (CH), 121.7 (CH), 121.4 (C), 114.3 (CH), 76.1 (CH), 68.0 (CH<sub>2</sub>), 47.0 (CH), 42.1 (CH<sub>2</sub>), 40.7 (CH<sub>2</sub>), 34.1 (CH<sub>3</sub>), 31.4 (CH), 31.1 (CH<sub>2</sub>), 26.1 (CH), 23.3 (CH<sub>3</sub>), 22.0 (CH<sub>2</sub>), 20.8 (CH<sub>2</sub>), 19.2 (CH<sub>2</sub>), 16.2 (CH<sub>3</sub>), 13.9 (CH<sub>3</sub>). Anal. calcd. for C<sub>36</sub>H<sub>42</sub>O<sub>7</sub>: C, 73.70; H, 7.22%. Found: C, 73.67; H, 7.24%.

CLCs **MnB4OB** (*n* = 2, 3, 4, 5, 6, 7, 8) were prepared from **MnB-OH** (*n* = 2, 3, 4, 5, 6, 7, 8) and 4-butoxybenzoic acid as described for the synthesis of **M/B4OB**. The detailed data of other CLCs **MnB4OB** were listed in ESI.

### 3. Results and discussion

#### 3.1. Elucidation of molecular structures

The synthetic routes of CLCs **MnB4OB** (*n* = 1-8) are illustrated in Scheme 1 and the last synthetic step of these compounds is esterification reaction. Except for varying length and parity of the connecting alkanedioxyloxy group, they possess similar structures with biphenyl

benzoate as mesogenic core, which was surrounded by a 4-butoxybenzoyl on one side and a chiral menthyl on the other side. The chemical structures of these intermediates and corresponding target compounds were confirmed by FT-IR and  $^1\text{H}$  NMR spectroscopic techniques.

The FT-IR spectrum of intermediate **M/B-OH** and CLC **M/B4OB** are illustrated in Figure 1. In the spectrum, we can see that the hydroxyl stretching absorption band at  $3515\text{ cm}^{-1}$  of intermediate **M/B-OH** disappear, while ester stretching bands at  $1747$ ,  $1724\text{ cm}^{-1}$  of **M/B-OH** move to  $1740$ , and  $1732\text{ cm}^{-1}$  for **M/B4OB**. Two medium intensity bands around  $2956$  and  $2869\text{ cm}^{-1}$  are due to aliphatic  $\nu$  (C-H) asymmetric and symmetric stretching vibrations of methylene ( $-\text{CH}_2-$ ) group, and the stretching vibration at  $1606$  and  $1510\text{ cm}^{-1}$  are attributed to  $\nu$  (C = C) of benzene ring.

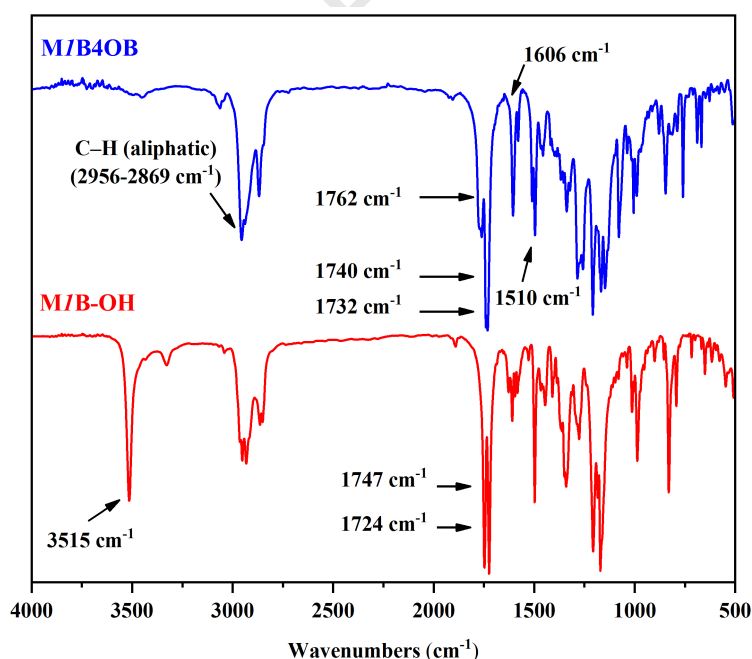


**Figure 1.** IR spectra of intermediate **M/B-OH** and CLC **M/B4OB**.

The structures of **M/B-OH** and CLC **M/B4OB** were also confirmed by  $^1\text{H}$  NMR spectra (Figure 2). In the spectra, aromatic ring proton peaks of intermediate **M/B-OH** are observed as multiplet around 7.59-7.48, 7.46-7.37, 7.20-7.06, 6.95-6.80 ppm. The signal

around 4.91 ppm in a singlet form corresponds to the proton of phenolic hydroxyl group. The signal around 4.81 ppm in a double triplet form observed corresponds to one proton of menthyl connecting to ester group. In contrast, hydrogenous chemical shift of aromatic ring of liquid crystal compound **M/B4OB** appear around 8.17-8.15, 7.62-7.57, 7.28, 7.19, and 6.98 ppm. Meanwhile, the signal of proton in menthyl connecting to ester group shifted to 4.82 ppm in a double triplet form. The signal around 4.06 ppm in a triplet form was observed due to the methylene of 4-butoxybenzoyl group. In addition, the signal around 3.62 ppm in a singlet form was observed, which ascribes to the methylene in malonyl group.

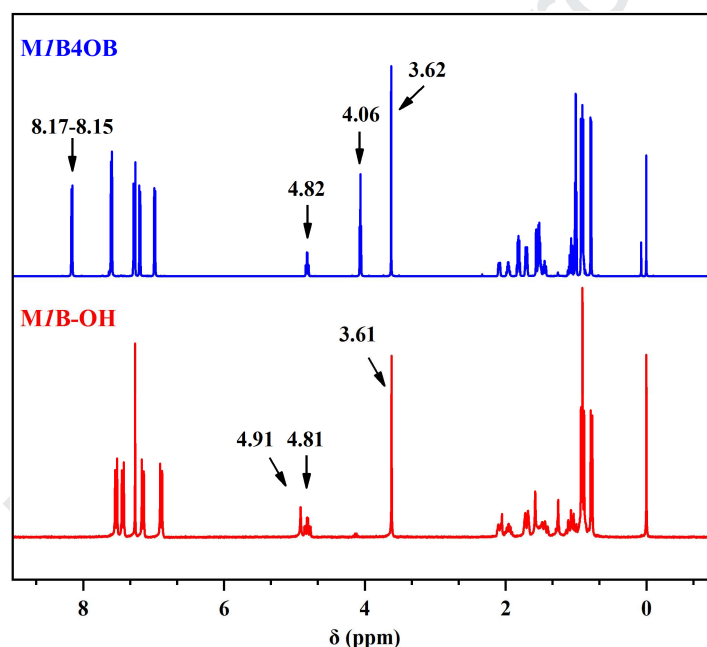


**Figure 2.**  $^1\text{H}$  NMR spectra of intermediate **M/B-OH** and CLC **M/B4OB**.

Other CLCs **MnB4OB** ( $n = 1-8$ ) are structurally identical except different spacer lengths, and their spectral results are almost similar. Through the FT-IR and NMR analysis, we can confirm that structures of the CLCs are in good agreement with the designs.

### 3.2. Thermal properties

In order to explore the influence of the linking spacer group on the mesomorphic behaviors of

the liquid crystalline compounds, these CLCs **MnB4OB** ( $n = 1$  to 8) were characterized by differential scanning calorimetry (DSC) and polarising optical microscope (POM). The transition temperatures and the corresponding enthalpies derived from DSC traces of the second heating-cooling cycles at a rate of  $10\text{ }^{\circ}\text{C min}^{-1}$  are given. Phase transition temperature and associated enthalpy changes of the synthesized compounds are given in Table 1. Typical DSC curves of **MnB4OB** ( $n = 2$  and 7) are shown as examples in Figure 3.

**Table 1.** Phase transitions and thermodynamic data for **MnB4OB**.

$n$	Phase transitions <sup>a</sup> ( $^{\circ}\text{C}$ ) (corresponding enthalpy changes; $\text{kJ mol}^{-1}$ ) <sup>b</sup>	
	Heating	Cooling
1	Cr142.9(71.98)Iso	Iso146.2(2.69)BPI/II142.2 $^{\circ}\text{C}$ N*117.5(60.55)Cr
2	Cr79.4(37.52)N*128.9(0.68)Iso	Iso127.1(0.66)BPI/II122.8 $^{\circ}\text{C}$ N*60.7(0.57)S <sub>A</sub> *5 3.4(32.18)Cr
3	Cr112.1(55.19)N*141.8(0.53)Iso	Iso139.9(0.60)N*95.7(4.67)S <sub>C</sub> *76.9(35.81)Cr
4	Cr102.2(62.23)N*134.7(0.41)Iso	Iso132.7(0.39)N*96.8(3.04)S <sub>C</sub> *69.9(1.37)S <sub>X</sub> * 61.1(16.65)Cr
5	Cr75.9(20.50)S <sub>C</sub> *100.5(4.46)N*134.0(0.9 9)Iso	Iso132.3(1.21)N*97.8(4.44)S <sub>C</sub> *72.9(2.44)S <sub>X</sub> * 58.8(11.47)Cr
6	Cr62.6(9.52)S <sub>X</sub> *76.9(2.03)S <sub>C</sub> *107.5(3.34) N*133.7(0.79)Iso	Iso131.8(0.62)N*104.7(3.18)S <sub>C</sub> *74.2(1.67)S <sub>X</sub> * *51.8(9.71)Cr
7	Cr62.0(8.73)S <sub>X</sub> *79.0(2.02)S <sub>C</sub> *110.4(2.86) N*135.5(0.71)Iso	Iso133.1(0.64)N*107.2(2.94)S <sub>C</sub> *75.7(1.85)S <sub>X</sub> * *51.8(8.40)Cr
8	Cr73.9(40.93)S <sub>C</sub> *102.1(4.23)N*125.0(0.1 0)Iso	Iso124.0(0.10)N*99.1(2.94)S <sub>C</sub> *73.9(2.27)S <sub>X</sub> * 42.6(5.91)Cr

<sup>a</sup>Cr: Crystal; N\*: chiral nematic phase; S<sub>A</sub>\*: chiral smectic A phase; S<sub>C</sub>\*: chiral smectic C phase; S<sub>X</sub>\* = chiral smectic X phase; Iso: isotropic phase.

<sup>b</sup>Values of enthalpy are given in brackets.  $n$  indicates the number of carbon atoms in the spacer chains.

<sup>c</sup>The transition temperatures were observed by POM at cooling rate of  $0.1\text{ }^{\circ}\text{C min}^{-1}$ .

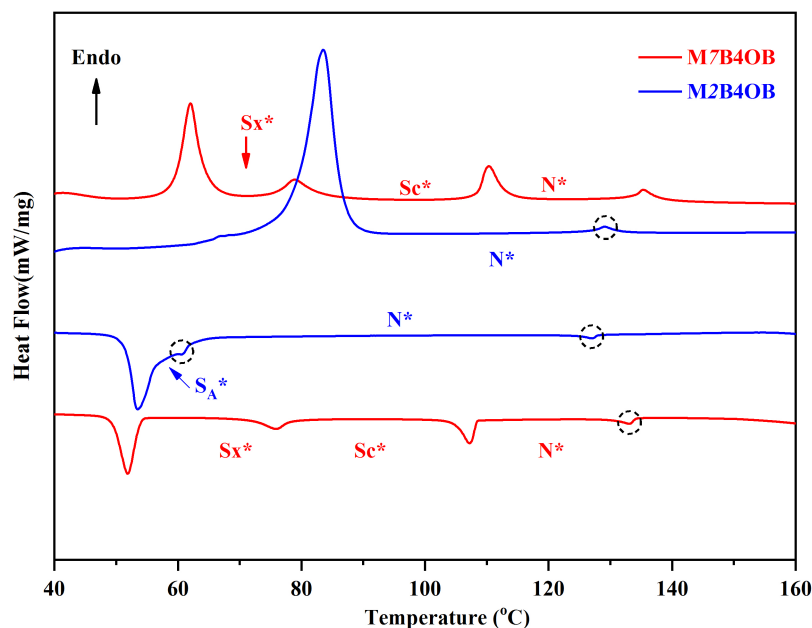


**Figure 3.** DSC curves obtained for the CLCs **M2B4OB** and **M7B4OB**.

As can be seen from Table 1, CLC **M1B4OB** only showed a melting transition and did not exhibit any mesophase on heating cycle due to the high melting point ( $T_m$ ). During its cooling process, CLC **M1B4OB** showed chiral nematic phase ( $N^*$ ), accordingly, CLC **M1B4OB** is monotropic. With spacer increasing the long spacer chains add flexibility to the rigid core structure, which tends to reduce melting points and allows liquid crystalline phases appear, so the higher members ( $n = 2-8$ ) show enantiotropic LC behavior. Upon heating, CLCs **M2B4OB**, **M3B4OB** and **M4B4OB** show  $N^*$  phases, and CLCs **M5B4OB**, **M8B4OB** reveal two mesophases, chiral smectic C ( $S_C^*$ ) and  $N^*$  phase. However, three mesophases of chiral smectic X phase ( $S_X^*$ ),  $S_C^*$  and  $N^*$  phases were observed for **M6B4OB** and **M7B4OB**. On cooling process, compounds **M2B4OB** and **M3B4OB** show an additional chiral smectic A ( $S_A^*$ ) or  $S_C^*$  phase respectively besides  $N^*$  phase. The other CLCs **MnB4OB** ( $n = 4-8$ ) exhibit three mesophase of  $N^*$ ,  $S_C^*$ ,  $S_X^*$  (an unknown chiral smectic X) from high to low temperature. The  $N^*$ ,  $S_A^*$ ,  $S_C^*$  and  $S_X^*$  phases were further confirmed by POM and XRD measurements. In addition, Table 1 shows that the clearing enthalpies of CLCs **MnB4OB** ( $n =$

2-8) give lower values irrespective to the length of the flexible spacers, which can attribute to the bulky nature of the menthyl group that enhances molecular biaxiality and reduces the change in order at the transition.

The relationship of phase transition temperatures (heating and cooling mode) with the number of carbon atoms ( $n$ ) for CLCs **MnB4OB** ( $n = 1-8$ ) is exhibited in Figure 4. It can be seen that as the spacing length with parity count  $n$  switches from odd to even the phase transition temperature reveals a regular changes. Melting temperatures ( $T_m$ ) and crystallization temperatures ( $T_{Cr}$ ) exhibited a modest odd-even effect as the parity of the spacer is varied and the odd members gave higher values than the corresponding even-parity ones. This indicates that the compound with odd spacer is more compact, which leads to a higher melting point than the even one as parity. Clearing temperature ( $T_c$ ) and Iso-N\* transition temperature ( $T_{Iso-N^*}$ ) also show the same variation pattern with melting point, the CLC with an odd spacer shows higher values than that with an even spacer, probably because even spacer CLCs are more twisted than the corresponding CLCs with odd spacer. These CLC compounds exhibit odd-even effect of the clearing temperature as the parity of the spacer is varied, which is similar to the odd-even effect of CLCs in terminal chain length [29] and LC dimers with various connecting spacer length [34,35]. However, there is no regular change in N\*-Sc\* transition temperature ( $T_{N^*-Sc^*}$ ) and Sc\*-Sx\* transition temperature ( $T_{Sx^*-Sc^*}$ ) with the increase of  $n$ . In addition, the S<sub>C</sub>\* phase appears as  $n$  greater than 4. This demonstrates that increasing the flexible spacers can favor the formation of S<sub>C</sub>\* phases, which is presumably due to the enhanced interlayer interactions derived from an increase of the spacers.

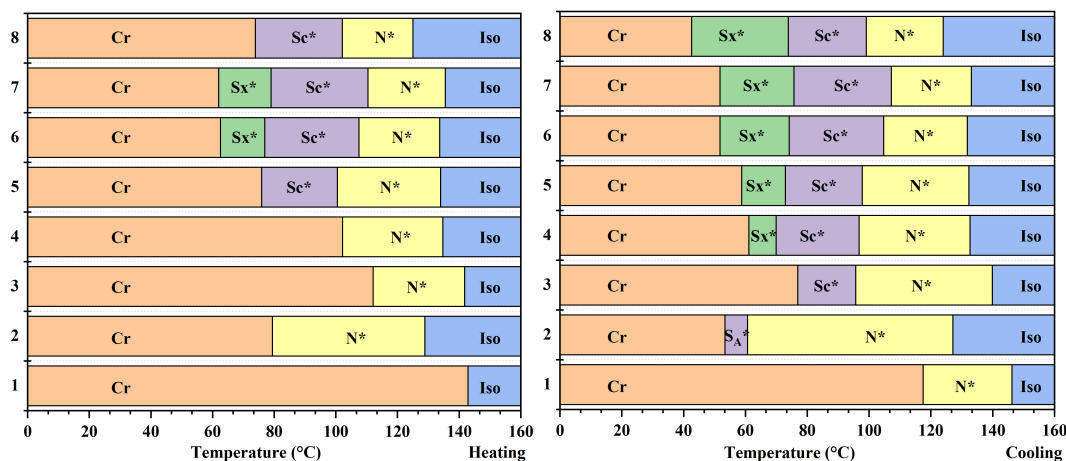


**Figure 4.** Phase diagram of compounds **MnB4OB** on heating and cooling cycles.

### 3.3. Optical textures

The mesomorphic transition temperatures observed by POM were consistent with the phase transition temperatures measured by DSC. Optical texture is one of the most effective means for identifying mesophase type. The optical textures of LC state were observed by means of POM with a hot stage, and some representative optical textures are given in Figure 5. On the heating course, the CLC **M1B4OB** directly melted to the isotropic phase without any mesophase and compounds **MnB4OB** ( $n = 2-8$ ) showed oily streaks texture (Figure 5a, b) in their N\* phase. The actual oily streaks can be seen as a network of defect lines dispersed in uniformly helical regions. The oily streaks texture disappeared until the sample entered into isotropic phase. Due to the enantiotropic behavior the  $S_C^*$  and  $S_X^*$  phases on heating course were further identified by their optical textures upon cooling. On cooling cycles, CLCs **M1B4OB** and **M2B4OB** revealed a platelet texture of BP (Figure 5c, d) and a broken focal conic texture (Figure 5e) of N\* phase, and an additional pseudo-isotropic texture of  $S_A^*$  phase for **M2B4OB**. Due to the enthalpy values of BP transition are too small to be detected by DSC. BPs of **M1B4OB** and **M2B4OB** exist over a very narrow temperature interval, about  $\sim 4$  °C because of the thermodynamic disruption. In addition, the other CLCs present an N\*

phase with a focal conic texture (Figure 5f) and  $S_C^*$  phase with a cloudy texture (Figure 5g). Here, the dull-greyish/cloudy patterns of  $S_C^*$  phase stemmed from the homeotropic orientation of the mesogens, which obviously suggested a layered structure of the phase. It is well known that if the helix axis of the  $S_C^*$  phase propagates along the direction of light (optic axis), then a greyish/cloudy textural pattern can be seen. When compounds **MnB4OB** ( $n = 4, 5, 6, 7, 8$ ) cooled further from the  $S_C^*$  phase, they exhibited another more ordered untypical texture (Figure 5h) of  $S_X^*$  phase. The more ordered  $S_X^*$  phase was proved by X-ray diffraction. Cooled the sample continuously, crystalline phase took place and mesophase disappeared.

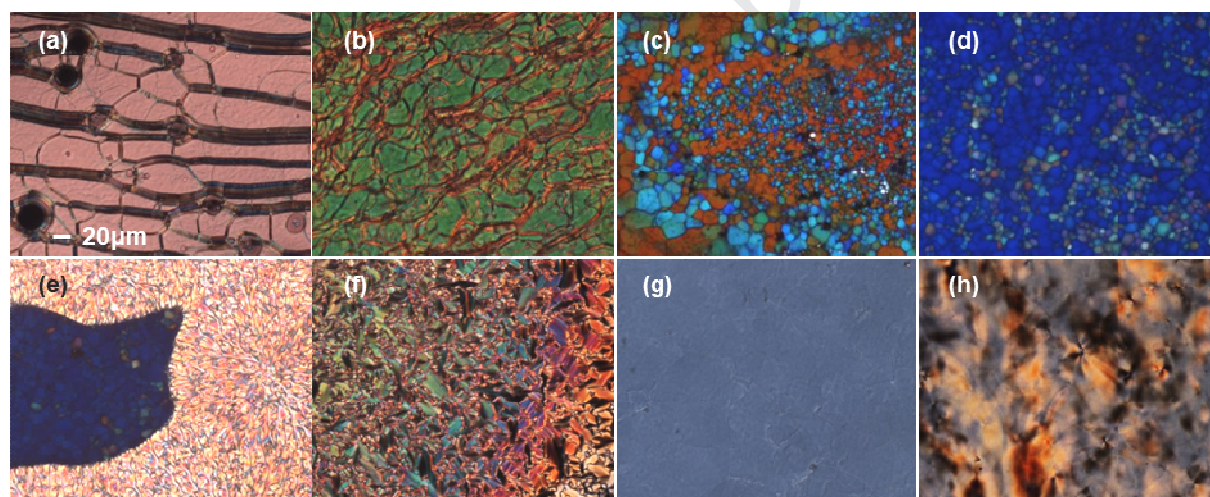


**Figure 5.** Photomicrographs of optical textures seen under POM for the liquid crystal phases of **MnB4OB** series: (a) oily streaks texture of  $N^*$  phase on heating to 107.1 °C for **M2B4OB**; (b) oily streaks texture of  $N^*$  phase on heating to 105.0 °C for **M5B4OB**; (c) a platelet texture of BPI/II on cooling to 146.1 °C for **M1B4OB**; (d) a platelet texture of BPI/II on cooling to 126.8 °C for **M2B4OB**; (e) broken focal conic textures with BPI/II texture of  $N^*$  phase on cooling to 122.5 °C for **M2B4OB**; (f) focal conic textures of  $N^*$  phase on cooling to 131.9 °C for **M7B4OB**; (g) cloudy texture of  $S_C^*$  phase on cooling to 102.0 °C for **M7B4OB**; (h) untypical texture of  $S_X^*$  phase on cooling to 61.5 °C for **M7B4OB**.

Notably, only CLCs **M1B4OB** and **M2B4OB** reveal a platelet texture composed of red, green and blue plates on slow cooling from the isotropic phase, which suggests the existence of a cubic BPI/II. The alluring and beautiful mesophase originates mainly from their

self-organized three-dimensional photonic crystal structure. With typical lattice spacing on the order of several hundred nanometers, selective Bragg reflection could be any color positioned in the visible region, and the corresponding wavelength is related to the lattice plane. The theoretical and experimental work has demonstrated that CLCs of short pitch could form up to three distinct BPs at the transition from isotropic phase to the N\* phase. Moreover, the double twist tube of BPs has been shown theoretically to be more stable than the single twist structure of the N\* phase at a higher temperature. In such a configuration, the energy can be further lowered by allowing twist in all directions perpendicular to the local director. In addition, we have also found that the chiral menthyl location with respect to the rigid core is important in determining the formation of BPs. When  $n$  is greater than 2, no BPs are formed for CLCs **MnB4OB** ( $n = 3-8$ ).

### **3.4. The selective reflection of light**

The planar oily streak texture of the N\* phase in heating exhibits one of the important optical phenomena, namely selective reflection. If the pitch length is of the order incident white light wavelength, then colors are selectively reflected. In general, the selective reflection wavelength depends on the molecular chirality and ordering of the molecules within the phase. The maximum wavelength ( $\lambda_m$ ) of the selective reflection is defined by Bragg Equation,  $\lambda_m = nP$ , where  $P$  is the pitch length of the helical structure and  $n$  is the average refraction index of the LCs. Importantly, helical pitch is temperature dependent; thus, the color of the reflected light varies with temperature.

In this work, the property of selective reflection in the N\* phase was examined with the help of UV/Vis spectra equipped with a hot stage. Only CLC **M2B4OB** selectively reflected visual light on heating, since  $P$  length of the N\* phase is of the order of the wavelength of

incident white light. Figure 6 shows the UV/Vis spectra of N\* phase for CLC **M2B4OB** obtained during heating cycles. Overall, it can be seen that blue shift of the maximum reflection wavelength ( $\lambda_m$ ) occurs as the temperature increases. Furthermore, their inherent reflection peak intensities are gradually weakened. According to the Bragg Equation, the rise of temperature leads the helical structure to twist and reduces the  $P$  value. So, with increasing temperature a blue shift of  $\lambda_m$  is observed and the reflection color varies from red to green (inset in Figure 6). In addition, the incident light beam will be split into its two circularly polarized components by the helical structure. One of the circularly polarized components will pass through the specimen, whereas the other component will be reflected. The component that is reflected has the same rotation sense as that of the screw direction of the helix.

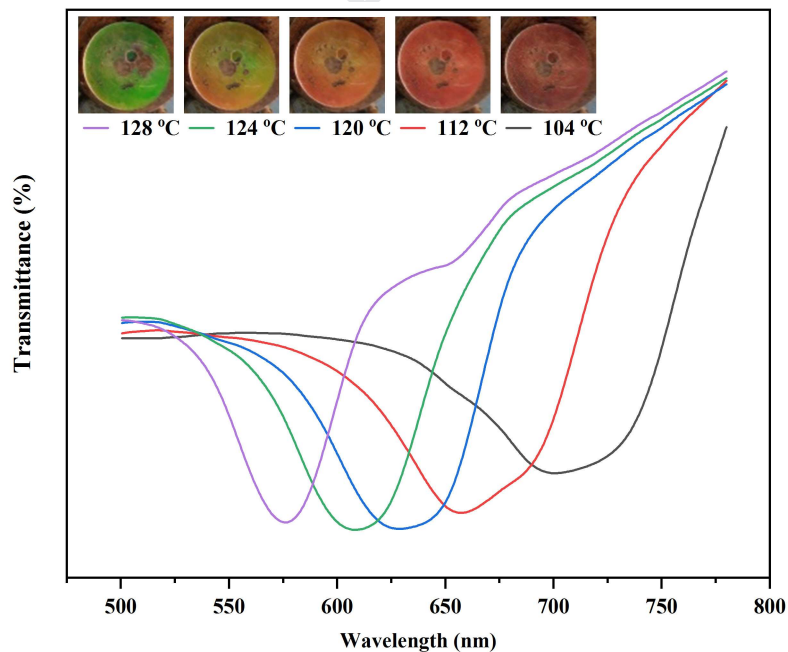


**Figure 6.** UV/Vis spectra of **M2B4OB** at N\* phase temperature range

As the length of the spacer increases, when  $n \geq 3$ , the pitch length of the N\* phase of this series CLCs is out of the order of the wavelength of white light, so no selectively reflection appears. Selective reflection in the visible range also requires a small pitch  $P$  for CLCs, so

BPs and selective reflection in the visible range are often observed for highly chiral mesogen. BPLCs normally show iridescent color in their N\* phase on heating process.

### 3.5. XRD studies

XRD analysis presented a complementary evaluation of the phases observed by DSC and POM, giving additional information about their structural parameters. In the cooling cycle, CLCs **M<sub>n</sub>B4OB** (n = 4-8) reveal a similar phase transition sequence of Iso-N\*-S<sub>C</sub>\*-S<sub>X</sub>\*-Cr. Thus **M7B4OB** was performed as an example for XRD measurement at the same cooling temperature operated by POM observation in order to get further insight into the mesophase structures. The diffraction patterns in the mesophase obtained on cooling from their isotropic phases. The intensity versus 2θ plots derived from the diffraction patterns of **M7B4OB** are shown in Figure 7. In the cooling scan, only a diffused peak at 2θ = 19.8° (*d*-spacing 4.48 Å) at 131.0 °C was observed. For this phase, focal conic textures were observed by POM. Therefore, combining XRD with POM, we can confirm that this phase is assigned as the N\* phase.

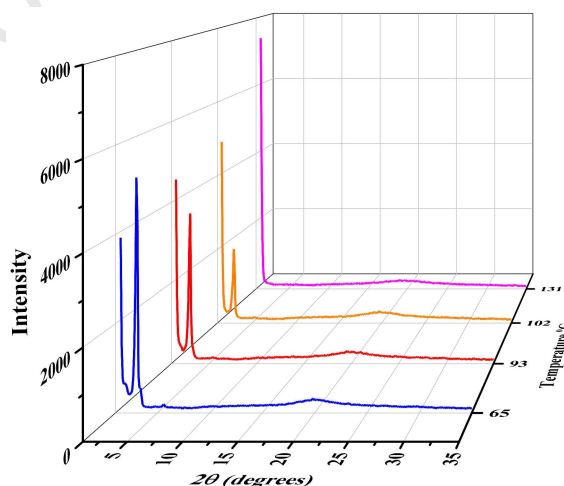


**Figure 7.** X-ray diffraction profiles for **M7B4OB**.

When cooled to 102 °C, the small-angle XRD scattering diffraction pattern showed one

strong reflection at  $2\theta = 2.9^\circ$  (d-spacing 30.43 Å), together with a diffused peak at  $2\theta = 19.8^\circ$  (d-spacing 4.48 Å). The sharp reflection in the small angle region indicates smectic layer arrangement of LC molecules. The theoretical molecular length ( $l$ ), calculated by the method of Chem 3D is about 35.85 Å. The  $d/l$  ratio of **M7B4OB** at 102 °C is 0.85, and which noted that the LC molecules tilt arrangement of  $S_C^*$  mesophase and the tilt angle ( $\alpha$ ), was calculated to be  $31.79^\circ$  from the equation  $\alpha = \cos^{-1}(d/l)$ . This identified that the cloudy texture in the mesophase observed by POM is  $S_C^*$  phase. The tilt angle in smectic  $C^*$  increases with the decrease of temperature. When cooled to 93 °C, the small-angle XRD scattering diffraction pattern showed one strong reflection at  $2\theta = 3.0^\circ$  (d-spacing 29.42 Å) and the tilt angle ( $\alpha$ ) was  $34.85^\circ$ . On further cooling to 65 °C, in addition to increase strength a reflection in the small angle is also located at  $2\theta = 3.0^\circ$ , and it is the same to the reflection at 93°C. The increase in reflection strength implies a more orderly arrangement of LC molecules. And combining DSC with POM results, a more ordered  $S_X^*$  mesophase was considered.

### 3.6 Molecules self-assemble in mesophase

(-)-Menthol is optically active and has three chiral centers. (-)-Menthol molecular asymmetry can impart chirality form to liquid-crystalline phases, which is manifested in the formation of helical ordering of the constituent molecules of the phase. The mesophase types of CLC **MnB4OB** series include Iso, BP,  $S_A^*$ ,  $S_C^*$ ,  $S_X^*$  and Cr phase and schematic representation of the molecular self-assembles is shown in Figure 8.

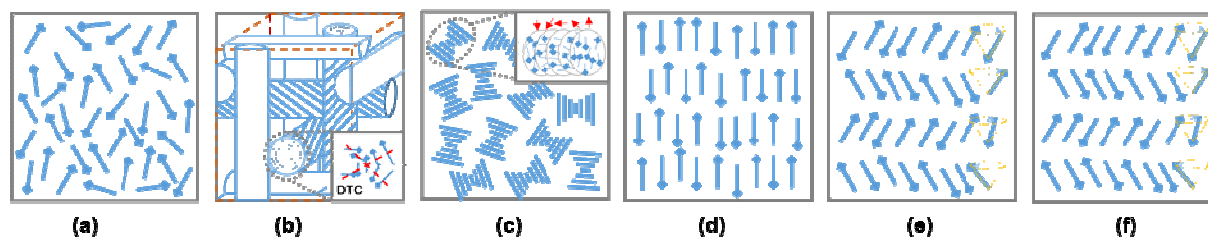


**Figure 8.** Schematic representation of the molecular arrangements in mesophase of CLC **MnB4OB**

The molecular arrangements are chaotic in the Iso state (Figure 8a). The N\* phase is a chiral phase, which spontaneously forms a macroscopic helical structure. As the temperature decreases, BP and the N\* phase appear. The chirality of (-)-menthyl in these compounds forces the mesogenic molecules to twist with respect to each other (inset in Figure 8b), resulting in the typical double twisted cylinder of BP (Figure 8b). The N\* phase (Figure 8c) also possesses a helix axis and consists of local nematic layers twisted continuously along the axis. Molecules in S<sub>A</sub>\* phase (Figure 8d) orient along the smectic layer normal, and the d-spacing is also almost equal to the theoretical molecular length. Helical smectic phases are also known to exist in the S<sub>C</sub>\* phase (Figure 8e) and in S<sub>C</sub>\* phase the chiral molecules tilt with respect to the layers normal. It is the precession of the tilt that gives rise to the macroscopic helical structure. Molecules arrangement of **MnB4OB** ( $n = 4-8$ ) in mesophase S<sub>X</sub>\* phase (Figure 8f) is similar to S<sub>C</sub>\* phase, except that it is more ordered than S<sub>C</sub>\* phase. The full phase transition sequence in cooling is an Iso-N\*-S<sub>C</sub>\*-S<sub>X</sub>\*-Cr process for compounds **MnB4OB** ( $n = 4-8$ ), an Iso-N\*-S<sub>C</sub>\*-Cr transition process for **M3B4OB**, an Iso-BP-N\*-S<sub>A</sub>\*-Cr transition process for **M2B4OB** and an Iso-BP-N\*-Cr transition process for **M1B4OB**.

Chiral menthyl location with respect to the rigid core has a great effect on the formation of BPs and mesomorphic behavior. As chiral menthyl location is closer to the rigid core ( $n < 3$ ), chiral menthyl lead molecules into DTC arrangement in BP interval for **M1B4OB** and **M2B4OB**. However, as the distance between the chiral center and core further increases ( $n \geq 3$ ) from **M3B4OB** to **M8B4OB**, menthyl is not powerful enough to make the molecular arrangement in DTC structure and only N\*, S<sub>C</sub>\* and S<sub>X</sub>\* phases form. This is because that

when the chiral center is closer to the core, the  $P$  of the helix becomes shorter, therefore, the chirality increases and BPs is formed [36]. In other words, when  $P$  exceeds a critical value,  $P_c$ , then BPs no longer exists.

#### 4. Conclusions

A series of CLC compounds was synthesized and characterized by modifying the position of chiral (-)-menthyl in relation to the mesogenic core. The CLC compound **M1B4OB** was monotropic LC, however the other members show enantiotropic LC behaviors. Melting temperatures ( $T_m$ ), clearing temperature ( $T_c$ ), Iso-N\* transition temperature ( $T_{\text{Iso-N}^*}$ ) and crystallization temperatures ( $T_{\text{Cr}}$ ) exhibit an odd-even effect as the parity of the spacer varied and the odd members show higher values than the corresponding even-parity CLCs. In addition, the position of chiral (-)-menthyl in relation to core has a great effect on the formation of BPs and mesomorphic behaviors. CLCs **M1B4OB** and **M2B4OB** revealed BPs with DTC structure. Increasing the length of the flexible spacers tended to favor the development of smectic phase. On cooling cycles, CLCs **M $n$ B4OB** ( $n = 4, 5, 6, 7, 8$ ) present a phase transition sequence from high to low temperature as: Iso-N\*-S<sub>C</sub>\*-S<sub>X</sub>\*-Cr.

#### Disclosure statement

No potential conflict of interest was reported by the authors.

#### Funding

This work was supported by the National Natural Science Foundation of China (31560268, 21702026), Fundamental Research Funds for the Central Universities (N180705004,

N170504018), the Science and Technology Foundation of Liaoning Province (20170520185), Fujian Natural Science Foundation (2019J0106), scientific research fund project of Ningde Normal University (2018Y06, 2018T02, 2018Z02) and IRTSTFJ.

## References

- [1] J. W. Goodby, P. J. Collings, T. Kato, C. Tschierske, H. Gleeson and P. Raynes, *Handbook of liquid crystals: fundamentals*, ed. Wiley-VCH, Weinheim, Germany, **2014**, vol. 1.
- [2] T. Geelhaar, K. Griesar and B. Reckmann, 125 Years of liquid crystals-a scientific revolution in the home, *Angew. Chem. Int. Ed.*, **2013**, 52, 8798-8809.
- [3] C. Tschierske, Development of structural complexity by liquid-crystal self-assembly, *Angew. Chem., Int. Ed.*, **2013**, 52, 8828-8878.
- [4] C. Tschierske, Liquid crystal engineering-new complex mesophase structures and their relations to polymer morphologies, nanoscale patterning and crystal engineering, *Chem. Soc. Rev.* **2007**, 36, 1930-1970.
- [5] A. Yoshizawa, Material design for blue phase liquid crystals and their electro-optical effects, *RSC Adv.*, **2013**, 3, 25475-25497.
- [6] A. Mazzulla, G. Petriashvili, M. A. Matranga, M. P. De Santo and R. Barberi, Thermal and electrical laser tuning in liquid crystal blue phase I, *Soft Matter*, **2012**, 8, 4882-4885.
- [7] F. Castles, F. V. Day, S. M. Morris, D. H. Ko, D. J. Gardiner, M. M. Qasim, S. Nosheen, P. J. W. Hands, S. S. Choi, R. H. Friend and H. J. Coles, Blue-phase templated fabrication of three-dimensional nanostructures for photonic applications, *Nat. Mater.*, **2012**, 11, 599-603.
- [8] D. L. Johnson, J. H. Flack, P. P. Crooker, Structure and properties of the cholesteric blue

- phases, *Phys. Rev. Lett.* **1980**, 45, 641-644.
- [9] O. Henrich, K. Stratford, M. E. Cates, D. Marenduzzo, Structure of blue phase III of cholesteric liquid crystals, *Phys. Rev. Lett.* **2011**, 106,107801.
- [10] T. H. Lin, C. W. Chen, Q. Li, In anisotropic nanomaterials: preparation, properties, and applications; Li, Q., ed.; Springer: Dordrecht, **2015**; Ch. 9.
- [11] P. P. Crooker, In chirality in liquid crystals, ed. H. S. Kitzerow and C. Bahr, Springer, New York, **2001**, Ch. 7.
- [12] W. Cao, A. Munoz, P. Palffy-Muhoray, B. Taheri, Lasing in a three-dimensional photonic crystal of the liquid crystal blue phase II, *Nat. Mater.*, **2002**, 1, 111-113.
- [13] S. Yokoyama, S. Mashiko, H. Kikuchi, K. Uchida, T. Nagamura, Laser emission from a polymer-stabilized liquid-crystalline blue phase, *Adv. Mater.*, **2006**, 18, 48-51.
- [14] H. Y. Chen, J. Y. Chiou, K. X. Yang, Reversible and fast shift in reflection band of a cubic blue phase in a vertical electric field, *Appl. Phys. Lett.*, **2011**, 99, 181119.
- [15] H. Y. Chen, J. L. Lai, C. C. Chan and C.-H. Tseng, Fast tunable reflection in amorphous blue phase III liquid crystal, *J. Appl. Phys.*, **2013**, 113, 123103.
- [16] M. D. A. Rahman, S. Mohd, S. Balamurugan, Blue phase liquid crystal: strategies for phase stabilization and device development, *Sci. Technol. Adv. Mater.* **2015**, 16, 033501.
- [17] H. Kikuchi, M. Yokota, Y. Hisakado, H. Yang, T. Kajiyama, Polymer-stabilized liquid crystal blue phases, *Nat. Mater.* **2002**, 1, 64-68.
- [18] Y. Chen, S. T. Wu, Recent advances on polymer-stabilized blue phase liquid crystal materials and devices, *J. Appl. Polym. Sci.* **2014**, 131, 40556.
- [19] V. Padmini, P. N. Babu, G. G. Nair, D. S. S. Rao, C. V. Yelamaggad, Optically biaxial, re-entrant and frustrated mesophases in chiral, non-symmetric liquid crystal dimers and

- binary mixtures, *Chem. Asian J.*, **2016**, 11, 2897-2910.
- [20] P. P. Crooker, Plenary lecture, the blue phases-a review of experiments, *Liq. Cryst.* **1989**, 5, 751-775.
- [21] J. Yan, S. T. Wu, K. L. Cheng, J. W. Shiu, A full-color reflective display using polymer-stabilized blue phase liquid crystal. *Appl. Phys. Lett.* **2013**, 102, 081102.
- [22] I. Dierking, Textures of liquid crystals, Weinheim: Wiley-VCH; 2003.
- [23] Y. Y. Li, Y. H. Cong, H. S. Chu, B. Y. Zhang, Blue phases induced by rod-shaped hydrogen-bonded supermolecules possessing no chirality or mesomorphic behavior, *J. Mater. Chem. C*, **2014**, 2, 1783-1790.
- [24] C. K. W. Jim, J. W. Y. Lam, C. W. T. Leung, A. J. Qin, F. Mahtab and B. Z. Tang, Helical and luminescent disubstituted polyacetylenes: synthesis, helicity, and light emission of poly(diphenylacetylene)s bearing chiral menthyl pendant groups, *Macromolecules*, **2011**, 44, 2427-2437.
- [25] J. S. Hu, D. Li, W. C. Zhang, Q. B. Meng, Synthesis, structure, and properties of chiral liquid crystal monomers and polymers based on menthol, *J. Polym. Sci., Polym. Chem.*, **2012**, 50, 5049-5059.
- [26] J. S. Hu, X. F. Liu, Q. B. Meng, Y. Zhang, New chiral liquid crystalline monomers, polymers, and elastomers derived from menthol derivatives: synthesis and mesomorphism, *J. Mater. Sci.*, **2014**, 49, 1229-1239.
- [27] J. S. Hu, X. Zhang, Y. G. Jia, Q. B. Meng, Synthesis and phase behaviour of chiral liquid crystalline monomers based on menthyl groups, smectic polymers and cholesteric elastomers, *Liq. Cryst.*, **2012**, 39, 121-131.
- [28] Y. G. Jia, J. S. Hu, D. Li, Q. B. Meng, X. Zhang, Synthesis and phase behavior of chiral

- liquid crystalline polymeric networks derived from menthol, *High Perform. Polym.*, **2012**, 24, 673-682.
- [29]C. C. Luo, Y. G. Jia, B. F. Sun, F. B. Meng, The effect of chain length in terminal groups on the mesomorphic behavior of novel (-)-menthol-based chiral liquid crystal compounds with a blue phase. *New J Chem.*, **2017**, 41, 3677-3686.
- [30]C. C. Luo, Y. G. Jia, K. M. Song, F. B. Meng, J. S. Hu, The effect of terminal alkoxy chain on mesophase behaviour, optical property and structure of chiral liquid crystal compounds derived from (-)-menthol. *Liq. Cryst.*, **2017**, 44, 2366-2378.
- [31]C. C. Luo, S. L. Sun, Y. S. Wang, F. B. Meng, J. S. Hu, Y. G. Jia, The effect of various functional groups on mesophase behavior and optical property of blue phase liquid crystal compounds based on (-) menthol [J], *J. Mol. Liq.*, **2018**, 269, 755-765.
- [32]Z. X. Zhu, C. C. Luo, J. W. Wang, J. S. Hu, Y. G. Jia, Synthesis and properties of (-)-menthol-derived chiral liquid crystals by introducing adipoyloxy spacer between mesogenic core and chiral menthyl [J], *Liq. Cryst.*, **2018**, 45, 1525-1534.
- [33]C. C. Luo, Q. L. Meng, J. W. Wang, G. Y. Yan, Y. G. Jia, Effect of spacer length on mesomorphic behaviours of chiral liquid crystal compounds containing (-)-menthyl [J], **2018**, 45, 1760-1770.
- [34]C. V. Yelamaggad, N. L. Bonde, A. S. Achalkumar, D. S. S. Rao, S. K. Prasad, A. K. Prajapati, Frustrated liquid crystals: synthesis and mesomorphic behavior of unsymmetrical dimers possessing chiral and fluorescent entities. *Chem. Mater.*, **2007**, 19, 2463-2472.
- [35]G. Shanker, C. V. Yelamaggad, Synthesis and thermal behavior of chiral dimers: occurrence of highly frustrated and cholesteric liquid crystal phases. *New J. Chem.*, **2012**,

36, 918-926.

[36]J. W. Goodby, Chirality in liquid crystals. *J. mater. Chem.*, **1991**, 1, 307-318.

Journal Pre-proof

## Highlights

Eight novel CLCs **M<sub>n</sub>B<sub>4</sub>OB** were synthesized by varying the distance of chiral (-)-menthyl in relation to the core.

The position of the chiral (-)-menthyl relative to the core determined whether the BPs can be formed.

Only CLCs **M<sub>1</sub>B<sub>4</sub>OB** and **M<sub>2</sub>B<sub>4</sub>OB** with short spacer displayed blue phase.

As the spacer length and parity increasing an odd-even effect was observed.

# The effect of the position of chiral (-)-menthyl on the formation of blue phase and mesophase behavior in biphenyl-benzoate liquid crystals

Zhang-Pei Chen<sup>1</sup>, Xin-Jiao Wang<sup>1</sup>, Ling-Xin Meng<sup>1</sup>, Ji-Wei Wang<sup>2,3\*</sup>, Ying-Gang Jia<sup>1\*</sup>

<sup>1</sup>*Department of Chemistry, College of Science, Northeastern University, Shenyang, 110819, P.*

*R.China*

<sup>2</sup>*Fujian Provincial Key Laboratory of Featured Materials in Biochemical Industry, College of*

*Chemistry and Materials, Ningde Normal University, Ningde, 352100, P. R. China*

<sup>3</sup>*Fujian Province University Engineering Research Center of Mindong She Medicine, College of*

*Chemistry and Materials, Ningde Normal University, Ningde, 352100, P. R. China*

## Disclosure statement

No potential conflict of interest was reported by the authors.